Monte Carlo investigation of the resonating-valence-bond ground state and a lattice statistical model

Bill Sutherland
Department of Physics, University of Utah, Salt Lake City, Utah 84112
(Received 28 December 1987)

We have suggested that the properties of the resonating-valence-bond (RVB) ground state can usefully be studied first by a correspondence with a lattice statistics model, and second by embedding this RVB point into a larger family of lattice statistical models—the loop gas. The nature of this loop gas—correlations, phase transitions, and order parameters—is studied in this paper by means of Monte Carlo techniques, on lattices of up to 4608 sites or 9216 bonds. An ordered phase is identified with divergent susceptibility and an order parameter which has the topology of a circle. Since the model is two dimensional, the phase transition is expected to be of Kosterlitz-Thouless (KT) type. The RVB point is within this ordered KT phase.

I. INTRODUCTION

Anderson and co-workers[1-3] have proposed that a resonanting-valence-bond (RVB) ground state may be applicable to the new high-temperature superconductors. This RVB state is an old idea, and visualizes the ground state of the electronic system as a quantum fluid of singlet pairs. The number of possible ways of pairing the electrons, or equivalently of orientating the singlet pairs on a lattice of $2N$ sites, is very large—exponential in N—and thus the ground state is a superposition over a very large number of nonorthogonal spin-pair basis states. In the new materials for which the RVB is thought to be applicable, the layered structure and highly anisotropic conductivity lead us to consider a two-dimensional RVB state.

We have made a theoretical effort[4,5] to understand the nature of the two-dimensional RVB state, and excitations from this ground state. In Ref. 4, we developed an exact correspondence of the correlations in the RVB ground state to the correlations in a lattice statistical problem. We have embedded this RVB point in a more general lattice statistical model[5]—the so-called "loop gas"—essentially by varying the ratio of diagonal to off-diagonal terms in the wave-function normalization by means of a fictituous activity of fugacity. We then argued that this more general loop gas has a phase transition, with two phases—a critical phase and an ordered phase.

The RVB point was sufficiently near the phase boundary that it was not immediately clear in which phase it might lie. In order to determine the nature of the RVB point, we have made Monte Carlo (MC) calculations on both the RVB and loop gas problems, using lattices with up to 4608 lattice sites or 9216 bonds. We find the following. First, the order parameter of the loop gas in the "ordered" phase is topologically like that of a planar x-y model, and by well-known theorems,[6,7] cannot have true long-range order in two dimensions. Instead, the phase transition is of the type that has become known as a Kosterlitz-Thouless[8] (KT) transition with a divergent susceptibility in the ordered or KT phase, but no long-range order. Second, the RVB point is in this ordered or KT phase. We believe that these facts offer a novel mechanism for superconductivity, and therefore presented a possible scenario for superconductivity in the RVB state.[9]

II. THE ORDER PARAMETER

Let us describe the loop gas model. The partition function is given by

$$Z(x,y)=\sum_c x^{P_2} y^{P'} ,$$

Here c is a loop covering on a square lattice. This means that closed loop are placed on the bonds between nearest neighbors of a two-dimensional square lattice, so that every site is on exactly one loop. The loops do not intersect or touch. We do allow loops of length 2 and zero area, corresponding to the diagonal terms in the normalization; there are P_2 of these. Otherwise the loops never retrace themselves, have finite area, and correspond to the off-diagonal terms in the normalization; there are P' of these. The parameters x and y are activities or fugacities which allow us to recover the entropy for given values of the thermodynamic variables P_2 and P'. A lattice of "size" N has $2N$ sites, $4N$ bonds, and the total length of all the loops is $2N=2P_2+P'$. The lattice is then wound on a torus, so that doubly periodic boundary conditions are imposed in directions parallel to the diagonals of the square lattice—or perhaps more properly, a diamond lattice. The RVB point is $x=2$, $y=4$, and the wave-function normalization $\Psi^+\Psi$ is proportional to the partition function at the RVB point. A typical configuration from the MC calculation at the RVB point is shown in Fig. 1.

The ordered phase is stabilized by $y\to\infty$, and it is to this limit that we shall now go understand the order parameter. (The parameter y is analogous to inverse temperature.) In this limit we make the number of loops of nonzero area P' as large as possible; this mean $N/2$ square loops each of length 4. In Fig. 2(a) we show such an ordered phase of squares "crystallized" onto one of

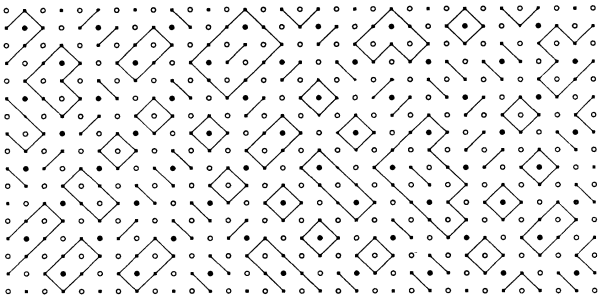

FIG. 1. This is an instantaneous configuration in a Monte Carlo simulation of the loop gas at the RVB point for a lattice of 256 sites and periodic boundary conditions. The dimers are actually zero-area loops of length 2. The initial configuration was a superlattice of squares on the faces indicated by solid circles.

four equivalent superlattices. The other possible phases are given by translations along the vertical and diagonal directions as shown and labeled in Fig. 3. Indeed, Fig. 3 shows a unit cell of the ordered superlattice. This unit cell contains 8 sites, 8 faces, and 16 bonds each grouped into four classes and appropriately labeled. (The lattice should contain a multiple of this unit cell and thus N should be a multiple of 4. In fact, we consider only doubly periodic lattices with equal repeat distances in the two directions, so that we have $M\times M$ unit cell and $N=4M^2$. Then the number of sites is $8M^2$, the number of bonds is $16M^2$, the number of faces is $8M^2$, the number of bonds of each class is $4M^2$, and the number of links is $8M^2$.)

However, there are not just four pure phases, with a sharp phase boundary between different phases in a phase mixture. Instead, we can mix for instance phase A and B arbitrarily finely by shifting diagonal rows of squares, as shown in Fig. 2(b), with no cost in energy and no phase boundary. Thus there is a continuum of equilibrium states, with the topology of a circle, going from $A\rightarrow B\rightarrow C\rightarrow D\rightarrow A$. (This is analogous to the shear instability in two-dimensional "crystals.")

We may define the order parameter as follows. Consider the four classes of bonds as labeled 0,1,2,3 in Fig. 3. There are N bonds of each class. Let

$$N_\alpha=\sum_{j\in\alpha} N(j)$$

be the number of links of the loop covering on bonds of class α. Then $N(j)$, the number of links on bond j, is 0,1, or 2, so $N_\alpha=0,\ldots,2N$. Let us represent the fractional occupancy of class α bonds by links by the loop covering as $n(\alpha)$, where

$$n(\alpha)=2N_\alpha/N-1,\quad 3\geq n(\alpha)\geq -1\ .$$

These occupancies are normalized so that the four superlattices of squares at $y\rightarrow\infty$ are given by $[n(0),n(1),n(2),n(3)]=(+1,+1,-1,-1)$ for A; $=(-1,+1,+1,-1)$ for B; $=(-1,-1,+1,+1)$ for C; $=(+1,-1,-1,+1)$ for D as shown in Fig. 4. We also show in Fig. 4(b) the square curve for the $y\rightarrow\infty$ equilibrium states with $A\rightarrow B\rightarrow C\rightarrow D\rightarrow A$. We note the sum rule

$$\sum_\alpha n(\alpha)=0\ .$$

It is useful at this point to make a change of variables

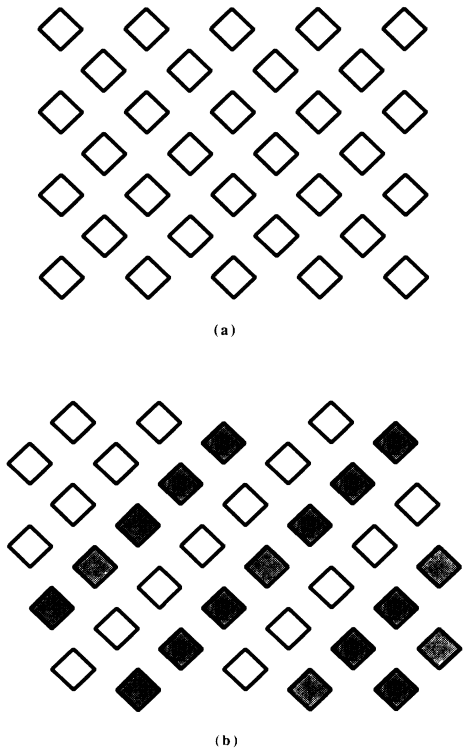

FIG. 2. (a) One of the four superlattices of squares for the loop gas as $y\rightarrow\infty$. (b) An intermediate equilibrium state for $y\rightarrow\infty$, halfway between the A and B phases. Shaded squares are on the A superlattice, while unshaded squares are on the B superlattice. (It could as well be the C and D phases.)

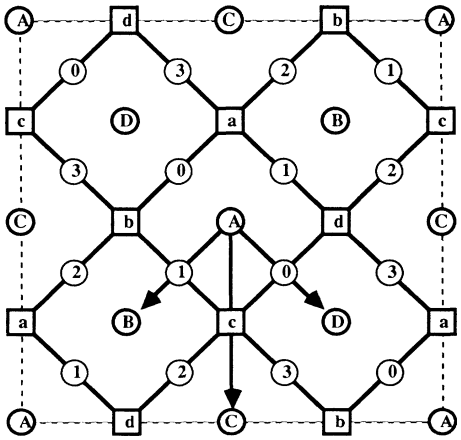

FIG. 3. The unit cell of the ordered superlattice. The classes of equivalent faces are labeled by bold circles, sites are labeled by squares, and bonds are labeled by light circles. The arrows indicate the transitions to take the A phase into the B, C, and D phases.

in order-parameter space, from the four dependent variables $n(\alpha)$ to the three independent variables u,v,w defined as

$$u=[n(0)+n(1)/2, \quad v=[n(0)+n(3)]/2 ,$$

$$w=[n(0)+n(2)]2$$

or

$$n(0)=u+v+w, \quad n(1)=u-v-w ,$$

$$n(2)=w-u-v, \quad n(3)=v-w-u .$$

Clearly the sum rule is satisfied. One final transformation to polar coordinates will prove useful:

$$r^2=u^2+v^2, \quad \tan(\theta)=v/u .$$

The Monte Carlo investigation in this paper is largely concerned with determining whether, and in what sense the order found for $y\rightarrow\infty$ persists for finite y.

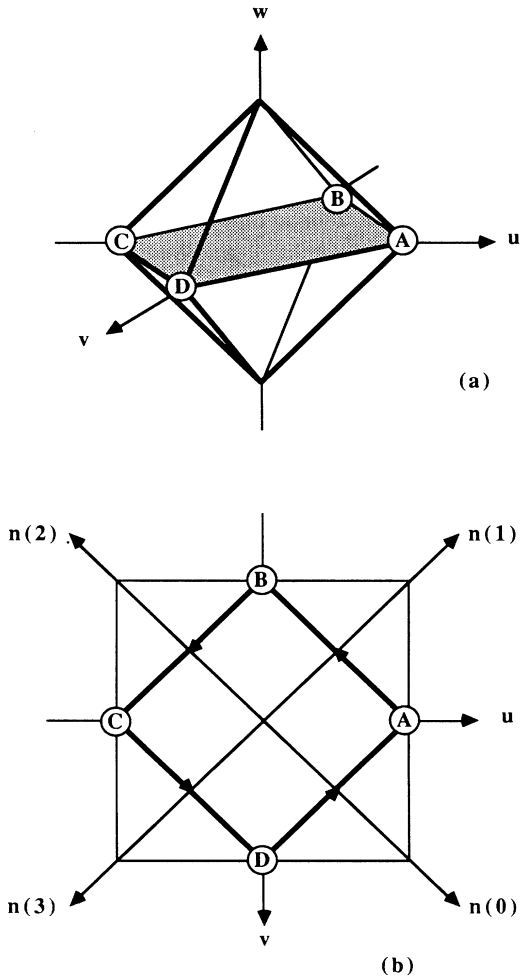

FIG. 4. The order parameter phase plane is shown. (a) The full u-v-w space. The shaded plane is the $w=0$ plane; the values of the order parameter contracts onto this plane. (b) The $w=0$ plane. The outer boundary is the allowed region. The bold directed square shows the phase boundary in the $y\rightarrow\infty$ limit, with the labeled corners giving the four periodic phases. The sense of the arrows shows a positive winding number of $+1$.

III. THE MONTE CARLO SCHEME

Before outlining the Monte Carlo (MC) calculation, we first need to derive some conservation laws. Let us consider a horizontal row of $4M$ bonds, which may be divided into M bonds of each of the four classes. This row connects with the next row of $4M$ bonds through a row of $2M$ sites. Let us suppose that from Ψ we have K dimers on the first row of bonds. These cover exactly K of the $2M$ sites, leaving $2M-K$ to be covered by the next row of dimers. Thus the partition function is symmetric if we reflect K about M, and therefore by the convexity of the free energy, we can as well evaluate the partition function in the "microcanonical" ensemble where the number of links or dimers from Ψ, and from Ψ^+, in *each* row and *each* column in the loop gas is exactly M.

The Monte Carlo calculation we use consists in making a transition from one loop gas configuration to another, by (1) picking a face at random from the $8M^2$ faces; (2) looking to see if there is a pair of dimers from either Ψ or Ψ^+ located on a pair of opposite edges of the face; (3) moving this pair of dimers from the original pair of opposite edges, to the alternate pair of opposite edges of the face, with a transition rate determined by the usual Metropolis algorithm.[10]

It is the determination of the transition rates which is complicated. If the number of nonzero loops does not change, then the Boltzmann weights $x^{P}{}^{2}y^{P'}$ can be determined entirely by a local calculation which examines only the configuration of dimers about a face. However, when the edges of the face are occupied only by a pair of dimers from either Ψ or Ψ^+ located on a pair of opposite edges, one must trace the entire loop beginning from one dimer to see if the two dimers lie on the same loop or not; the transition rates will be different in the two cases. In rare cases, this can require us to walk a loop of length equal to the size of the entire system. In Fig. 5 we show those dimer configurations about a face which may possibly lead to a flip, along with the ratio R of the Boltzmann weight of the configuration after the flip, to the Boltzmann weight of the configuration before the flip. For the Metropolis algorithm—which we use—the transition rate is equal to the ratio of the Boltzmann weights if the ratio is less than one, and unity otherwise.

This scheme obviously keeps us within the microcanonical ensemble, since it can never change the number of dimers within a row or column. We have no doubts that all states within the microcanonical ensemble are accessible, although we have not proven it. As our initial configuration, we take the $y\rightarrow\infty$ limit of one of the four superlattices of squares. This guarantees that we are within the proper microcanonical ensemble.

Thus the basic transition is such a "flip" of a pair of dimers. (We call it a flip whether it is actually realized or not.) Then for an "update," we take an average of one flip per face, or $8M^2$ flips. For a "run", we fix x,y and the size of the system M. We then start with 1000 updates to bring the system to equilibrium, begin recording running averages for 1000 updates, store the result, begin new running averages, etc., and repeat for a total of 10 times. Then we keep x and the size of the system M con-

stant, while y is increased along a "heating" curve for another run, using the final configuration from the last run as the initial configuration of the new run.

We then made runs with x always fixed at 2, and $y=10,6,5,4,3,2,1$ for systems of $M=2,4,6,8,10,12$; and $y=4,3,2,1$ for $M=24$. (Remember, the number of sites is $8M^2$ and the number of bonds is $16M^2$.) A total of approximately 50 h of CPU time on a VAX785 computer was thus consumed.

IV. RESULTS: QUALITATIVE FEATURES

The Monte Carlo calculation picks systems of size N from an ensemble of such independent systems, by performing a random walk within the ensemble, with visitation times proportional to the Boltzmann weights. Thus an average over the walk of the MC calculation will converge to an ensemble average. Since we are in fact interested in the thermodynamic limit of large systems, when $N\rightarrow\infty$, a second limiting process will be necessary.

Let us use k to denote a system selected from the ensemble, with $k=1,\ldots,L$. Let the unnormalized weights be $\Omega(k)$. If q denotes an intensive thermodynamic parameter such as $n(\alpha)$, given by a system average over sites j in a system of size N as

$$q=\sum_j q_j/N \ ,$$

then let $q(k)$ and $q_j(k)$ be the value of q and q_j in system k of the ensemble. Thus, the thermodynamic value of q is the ensemble average $\langle q\rangle$ of q, given by

$$\langle q\rangle=\sum_k \Omega(k)q(k)/\sum_k \Omega(k)$$

$$=\left[N\sum_k \Omega(k)\right]^{-1}\sum_k\sum_j \Omega(k)q_j(k) \ .$$

Similarly, we can calculate the mean-square deviation

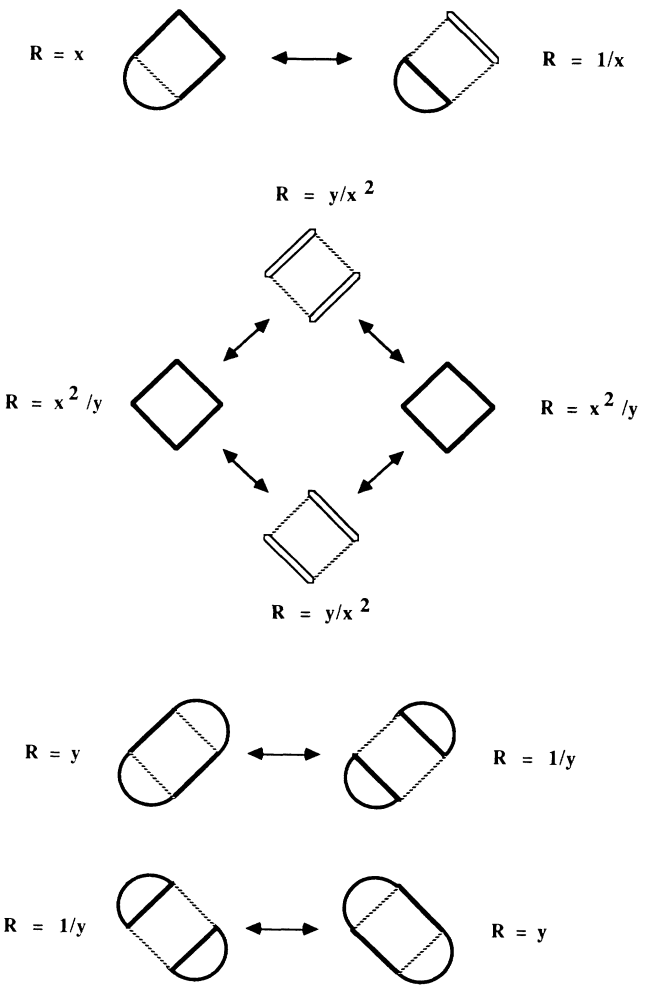

FIG. 5. Those dimer configurations about a face which may possibly lead to a flip, along with the ratio R of the Boltzmann weight of the configuration after the flip, to the Boltzmann weight of the configuration before the flip. This ratio R gives the transition rates. Double lines are a pair of dimers and dashed lines are empty bonds on the face; a curved semicircle represents a path of arbitrary length extending off the face and through the remainder of the lattice.

$$\langle(q-\langle q\rangle)^2\rangle=\langle q^2\rangle-\langle q\rangle^2=\sum_k \Omega(k)q^2(k)\Big/\sum_k \Omega(k)-\langle q\rangle^2$$

$$=\left[N^2\sum_k \Omega(k)\right]^{-1}\sum_k\sum_j\sum_{j'} \Omega(k)(q_j(k)-\langle q\rangle)(q_{j'}(k)-\langle q\rangle)$$

$$=N^{-2}\sum_j\sum_{j'} g_{qq}(j,j')\equiv\chi_{qq}/N \ .$$

In this expression, we have introduced the familiar pair-correlation function $g_{qq}(j,j')$ and susceptibility χ_{qq}. In the usual situation with translational invariance and rapid decay of correlations, $g_{qq}(j,j')=g_{qq}(j-j')$ so that χ_{qq} is intensive. For the loop gas the correlations decay very slowly, so the susceptibility may not converge in the thermodynamic limit. In any case, all quantities defined above are implicitly functions of the size N of the system.

However, in the MC calculation we not only get the moments of an intensive thermodynamic quantity q, but more generally the distribution function $P(q)$ is defined by

$$P(q)=\langle\delta(q-q')\rangle=\sum_k \Omega(k)\delta(q-q(k))\Big/\sum_k \Omega(k) \ .$$

Again this is an implicit function of the system size N. The previous moments of q are moments with respect to this distribution.

In this section we wish to discuss the qualitative nature of this distribution function when N is of a convenient size and the intensive thermodynamic parameter q is the set of proposed order parameters for the system: $n(\alpha)$, $\alpha=0,1,2,3$; or better u,v,w; or as we shall see, u,v or equivalently r,θ. Although not producing "numbers," such a study is well worth the time since it is certainly more rewarding than simply looking at a succession of pictures like Fig. 1 and at the same time will give us an idea of what numbers we should be calculating in Sec. V. (The pictures of Fig. 1 were, however, invaluable for debugging the program.)

The first qualitative feature of a MC run is that the distribution function $P(u,v,w)$ contracts onto the u-v plane with $\langle w\rangle=0$, and $\langle w^2\rangle=\chi_{WW}/N$. The numerical support for this will be presented in Sec. V; it is immediately apparent by eye. Thus, let us project down onto the u-v plane and consider the distribution function $P(u,v)$. For $w=0$, the allowed values of u and v are $-1\leq u\leq 1$, $-1\leq v\leq 1$. In Fig. 6, we plot a point in the u-v plane for each time that value of (u,v) was measured in a single MC run. The system size was $N=(14)^2=196$, or $M=7$. This value was chosen since the variables u and v change in steps of $2/N$, and with a screen resolution of $(200)^2$ pixels, this allows us to avoid any binning effects. Furthermore, for a reasonable MC run of 4000 points, this gives us a coverage of about 10%, so that the visual density of the scatter plot should give a good idea of the actual density $P(u,v)$. In Fig. 6, we show a succession of pictures at intervals of 1000 updates, for $x=2$ and $y=10$. Other values of y with $y\geq 3$ are qualitatively similar.

We note the following two features of this picture, most evident for the large value of y.[1] The points are most dense in a region with roughly the shape of the circumference of a circle. (2) As the number of points accumulate, they are distributed roughly uniformly around this circular region. Watching the points accumulate in time gives one the impression that the angle θ is performing a random walk.

In light of these qualitative features, we expect that the "order parameter" is planar in nature with the topology of a circle or U(1) symmetry, and since the lattice is two-dimensional, by well-known rigorous arguments there can be no long-ranged order, because of the strong fluctuations of the local angle θ of the order parameter. However, there can still be a Kosterlitz-Thouless type of phase transition characterized by a transition from a divergent to a finite susceptibility χ_{rr}. This interpretation will shape the analysis of Sec. V.

V. RESULTS: QUANTITATIVE FEATURES

We have already described how the Monte Carlo calculations were made; in this section we present the quantitative results. In light of the expected long-ranged power-law correlations, we decided to minimize the amount of evaluation and determine only the essentials, so that we might go to systems with linear dimensions of approximately 100 bond-lattice constants. (Previous calculations for the RVB state—an exact enumeration of dimer configurations—were limited to a 4×4 square lattice.[11]

This precludes the possibility of a complete evaluation of the correlation functions, for this would require us to walk each loop of a loop gas configuration. Also, the amount of data would be so large as to be unwieldy. (We did perform such a calculation on rather small systems of up to 128 sites, verifying that the RVB variational estimate of the Heisenberg antiferromagnet ground state remains about 4% above the best variational estimate

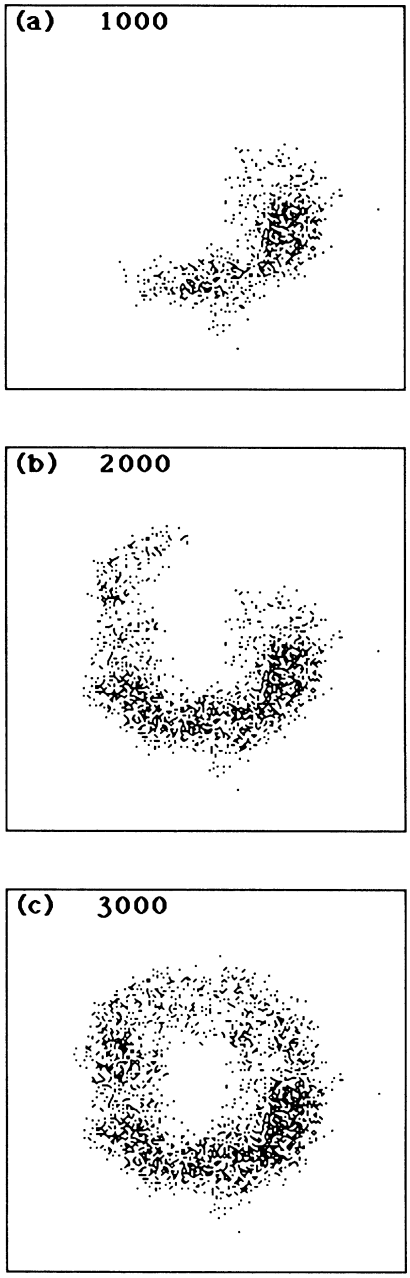

FIG. 6. We plot a point in the u-v plane for each time that value of (u,v) was measured in a single MC run. The system size was $N=(14)^2=196$, or $M=7$. We show a succession of three pictures taken at intervals of 1000 updates, for $x=2$ and $y=10$.

with other trial wave functions.

Instead, we chose to evaluate only four quantities: $\langle w \rangle$, $\langle w^2 \rangle$, $\langle r \rangle$, and $\langle r^2 \rangle$. First, we give in Fig. 7 a ln-ln plot of $\langle w^2 \rangle$ versus the system size N. Clearly these confirm our remark in Sec. IV that w is not an order parameter of the system but is simply an ordinary thermodynamic variable with equilibrium value $w=0$, and a susceptibility $\chi_{ww}(2,y)$ as shown in Fig. 8. There is no evidence for any anomaly as a function of y. (As we shall see in the next paragraph, the evaluation of $\langle w \rangle$ serves only as a check on the consistency of the MC calculation, since it is expected to vanish on general grounds.)

For the remaining two quantities, $\langle r \rangle$ and $\langle r^2 \rangle$ some interpretation is in order before we present the numerical results. The loop gas has geometric symmetries which in order parameter space translate into a dihedral symmetry D_4, or invariance if

$$w \to -w, \quad \theta \to -\theta \quad \text{or} \quad \theta \to \theta + \pi/2 .$$

Then for averages of the order parameters, by symmetry we will have

$$\langle u \rangle = \langle v \rangle = \langle w \rangle = 0$$

and

$$\langle w^2 \rangle = \chi_{ww}/N, \quad \langle u^2 \rangle = \langle v^2 \rangle = \chi_{rr}/(2N) ,$$

$$\langle uv \rangle = \langle vw \rangle = \langle wu \rangle = 0 .$$

These symmetries, however, strictly hold only in the limit of an infinite Monte Carlo run.

Let us examine the expression from Sec. IV for

$$\langle r^2 \rangle = \langle (u^2+v^2) \rangle = \chi_{rr}/N .$$

In fact, let us course grain the order parameter so that we define a local order parameter with components $u_j = r_j \cos(\theta_j)$, $v_j = r_j \sin(\theta_j)$. Then alternatively

$$\langle r^2 \rangle = \chi_{rr}/N = N^{-2} \sum_j \sum_{j'} \langle r_j r_{j'} [\cos(\theta_j)\cos(\theta_{j'}) + \sin(\theta_j)\sin(\theta_{j'}]\rangle$$
$$= N^{-2} \sum_j \sum_{j'} \langle r_j r_{j'} \cos(\theta_j - \theta_{j'}) \rangle .$$

Now the correlations in r can be expected to decay rapidly, so that

$$\langle r^2 \rangle = \chi_{rr}/N = \langle r \rangle^2 \sum_j \sum_{j'} \langle \cos(\theta_j - \theta_{j'}) \rangle / N^2 .$$

Finally, by the familiar arguments from spin-wave theory for the fluctuation in the local angle of the order parameter, we expect the pair correlation function for the angles to decay as a power of the separation $|j\text{-}j'|$. Defining an appropriate exponent η by

$$g_{\theta\theta}(j,j') = \langle \cos(\theta_j - \theta_{j'}) \rangle \to g_0 |j - j'|^{-\eta} .$$

we have the final result that

$$\chi_{rr} = \langle r \rangle^2 g_0 \sum_j |j|^{-\eta} \to [\langle r \rangle^2 g_0/(1-\eta/2)] N^{1-\eta/2} .$$

This expression only holds when χ_{rr} diverges with increasing N, or $\eta < 2$.

Thus, a ln-ln plot of $\chi_{rr} = N\langle r^2 \rangle$ as a function of N, for large N should give a straight line with either finite slope $1-\eta/2 > 0$, or zero slope and a finite susceptibility in the thermodynamic limit. The transition between these two kinds of behavior indicates a Kosterlitz-Thouless–type phase transition due to the unbinding of pairs of vortices with winding number $\Delta\theta/2\pi = \pm 1$. The intercept of such a plot might loosely be related to the magnitude of the length of the local order parameter $\langle r \rangle^2$.

After this lengthy prelude, in Fig. 9, we present such a

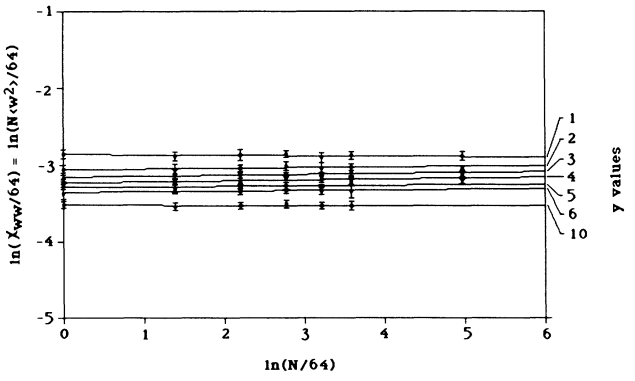

FIG. 7. ln-ln plot of susceptibility $\chi_{ww} = N\langle w^2 \rangle$ vs system size N. The straight line is a least-squares fit to the data for systems of size $N = 4(12)^2 = 576$ or less; i.e., all but the right-most set of points.

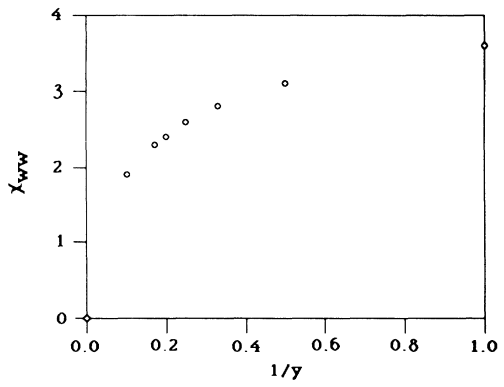

FIG. 8. A plot of the susceptibility χ_{ww} vs $1/y$ as determined from the data of Fig. 7.

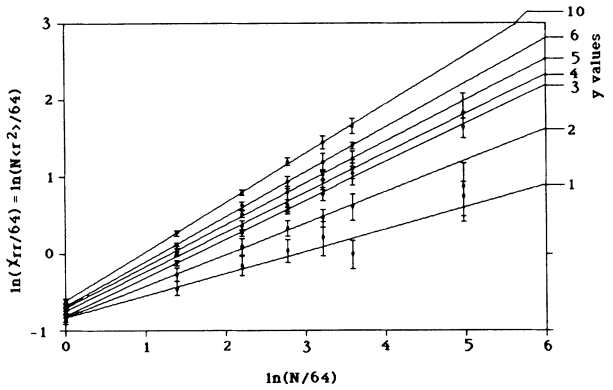

FIG. 9. ln-ln plot of susceptibility $\chi_{rr}=N\langle r^2\rangle$ vs system size N. The straight line is a least-squares fit to the data for systems of size $N=4(12)^2=576$ or less; i.e., all but the right-most set of points.

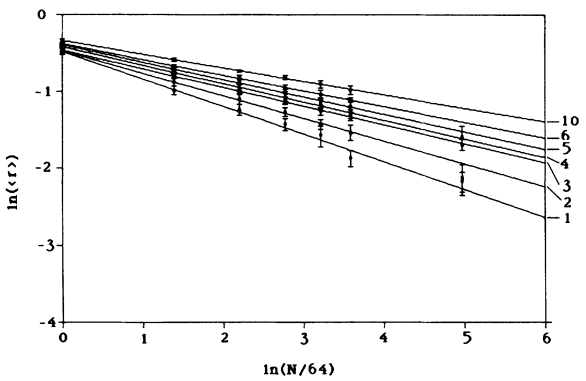

FIG. 11. This graph shows ln-ln plot of $\langle r\rangle$ vs system size N. The straight line is a least-squares fit to the data for systems of size $N=4(12)^2=576$ or less; i.e., all but the right-most set of points.

ln-ln plot of $\chi_{rr}=N\langle r^2\rangle$ versus N. The straight line is a least-squares fit to the data for systems of size $N=4(12)^2=576$ or less. For $y=1,2,3,4$ we calculated one more point for a system of size $N=4(24)^2=2304$, to see if the susceptibility started turning down, possibly to a finite value. Clearly for $y=3$ and 4 there is no evidence at all for the least deviation from a pure power law behavior for the susceptibility. On the contrary, for $y=1$ and 2 there is such a break, and the behavior is more complex with large fluctuations in the MC results. Thus, we claim that for the loop gas with $x=2$, there is a critical value of y—$3\geq y_c(2)\geq 2$— such that χ_{rr} diverges for $y>y_c(2)$, and χ_{rr} is finite for $y<y_c(2)$. This puts the RVB point $y=4$ well within the region where χ_{rr} diverges.

In Fig. 10, we show a plot of the exponent η as a function of $1/y$ as derived from those curves in Fig. 9 with $y\geq 3$, which show no sign of breaking from a straight line. Thus all values of η satisfy $\eta<1$, and the shape of the curve strongly suggests a critical value of η at the critical point with $\eta_c=1$.

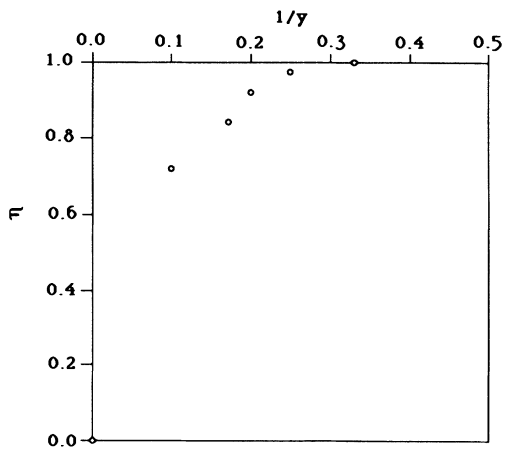

FIG. 10. This graph shows a plot of the correlation function exponent η vs $1/y$ as determined from the data in Fig. 9.

Finally, in Fig. 11 we give corresponding ln-ln plots of $\langle r\rangle$ versus N. We see, however, little additional physical information to be gained beyond that contained in Figs. 9 and 10.

VI. SUMMARY AND CONCLUSION

In conclusion, we have presented numerical evidence based on a Monte Carlo investigation, for the existence of a Kosterlitz-Thouless type of transition in the loop gas and RVB models. These two dimensional models have an order parameter with a U(1) symmetry, so that fluctuations of the local angle of the order parameter destroy any true long-range order, yet which still exhibit a phase transition into a phase characterized by a divergent susceptibility—the KT phase. This KT phase is believed to be characterized by bound pairs of vortices with winding numbers ± 1; the phase transition is thought to be due to the unbinding of the vortices. The RVB state is well within the KT phase, and the significance of this feature for the theory of high-temperature superconductors has been spelled out in an earlier paper by this author.[9].

We would, however, like to emphasize some significant differences from the usual Kosterlitz-Thouless transitions. First, as was emphasized in Ref. 5, the "high-temperature" or critical phase when $y\leq y_c<3$ for $x=2$ is a phase which also has power-law decay of correlations. In fact, as was pointed out long ago by Kasteleyn,[12] the identical susceptibility χ_{rr} for the exactly soluble dimer problem $y=0$, or $x=1$ and $y=2$ diverges. This is in contrast to traditional Kosterlitz-Thouless systems, where the correlation function decays exponentially and the susceptibility is finite in the "high-temperature" phase. (Of course, as argued in Ref. 5, spin-spin correlations do decay exponentially throughout the loop soup phase plane.) Second, we have found the critical value of η_c to be $\cong 1$, in contrast to the usual KT value of $\cong\frac{1}{4}$. In this respect, the loop gas resembles more closely the one-

dimensional Heisenberg-Ising model at the isotropic point $\Delta = -1$.

ACKNOWLEDGMENTS

The author would like to thank David Fitzjarrell and Michael Giddings for help with the computer programming; Tony Szpilka for providing an effective random-number generator; Ken Kubo and Tom Kaplan for guidance in devising the Monte Carlo scheme; Mahito Kohmoto and Sriram Shastry for suggestions; P. W. Anderson for an invitation to the Princeton RVB workshop, which inspired this investigation; and finally the National Science Foundation Grant No. DMR 86-15609 and the Physics Department of the University of Utah for financial support.

[1]P. W. Anderson, Science **235**, 1196 (1987).

[2]P. W. Anderson, G. Baskaran, Z. Zou, and T. Hsu, Phys. Rev. Lett. **58**, 2790 (1987).

[3]G. Baskaran, Z. Zou, and P. W. Anderson, Solid State Commun. **63**, 973 (1987).

[4]B. Sutherland, Phys. Rev. B **37**, 3786 (1988).

[5]B. Sutherland (unpublished).

[6]N. D. Mermin and H. Wagner, Phys. Rev. Lett. **17**, 1133 (1966).

[7]P. C. Hohenberg, Phys. Rev. **158**, 383 (1967).

[8]J. M. Kosterlitz and D. J. Thouless, J. Phys. C **6**, 1181 (1973).

[9]B. Sutherland (unpublished).

[10]N. Metropolis, A. W. Rosenbluth, A. H. Zeller, and E. Zeller, J. Chem. Phys. **21**, 1089 (1953).

[11]P. L. Iske and W. J. Caspers, Physica **142A**, 360 (1987).

[12]P. W. Kasteleyn, J. Math. Phys, **4**, 287 (1963).

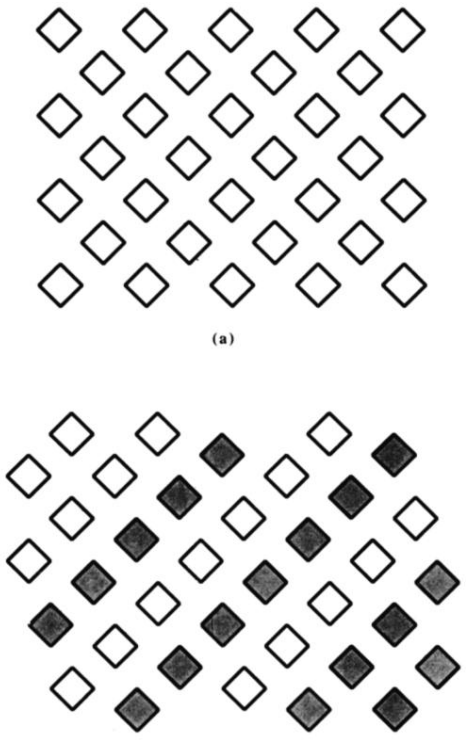

(a)

(b)

FIG. 2. (a) One of the four superlattices of squares for the loop gas as $y \to \infty$. (b) An intermediate equilibrium state for $y \to \infty$, halfway between the A and B phases. Shaded squares are on the A superlattice, while unshaded squares are on the B superlattice. (It could as well be the C and D phases.)

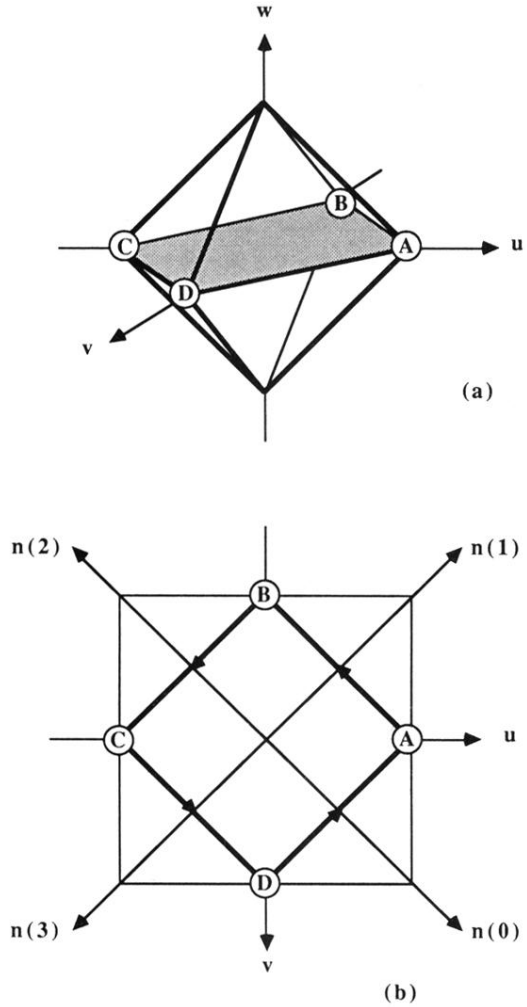

FIG. 4. The order parameter phase plane is shown. (a) The full u-v-w space. The shaded plane is the $w=0$ plane; the values of the order parameter contracts onto this plane. (b) The $w=0$ plane. The outer boundary is the allowed region. The bold directed square shows the phase boundary in the $y\rightarrow\infty$ limit, with the labeled corners giving the four periodic phases. The sense of the arrows shows a positive winding number of $+1$.